Towards the analytic characterization of micro and nano surface features using the Biharmonic equation

G. González Castro[a], R. Spares[a], H. Ugail[b], B. R. Whiteside[a], J. Sweeney[a]

[a] *School of Engineering, Design and Technology, University of Bradford, United Kingdom.*
[b] *Centre for Visual computing, University of Bradford, United Kingdom.*

Abstract

The prevalence of micromoulded components has steadily increased over recent years. The production of such components is extremely sensitive to a number of variables that may potentially lead to significant changes in the surface geometry, often regarded as a crucial determinant of the product's functionality and quality. So far, traditional large-scale quality assessment techniques have been used in micromoulding. However, these techniques are not entirely suitable for small scales . Techniques such as Atomic Force Microscopy (AFM) or White Light Interferometry (WLI) have been used for obtaining full three-dimensional profiles of micromoulded components, producing large data sets that are very difficult to manage. This work presents a method of characterizing surface features of micro and nano scale based on the use of the Biharmonic equation as means of describing surface profiles whilst guaranteeing tangential (C^1) continuity. Thus, the problem of representing surface features of micromoulded components from massive point clouds is transformed into a boundary-value problem, reducing the amount of data required to describe any given surface feature.The boundary conditions needed for finding a particular solution to the Biharmonic equation are extracted from the data set and the coefficients associated with a suitable analytic solution are used to describe key design parameters or geometric properties of a surface feature. Moreover, the expressions found for describing key design parameters in terms of the analytic solution to the Biharmonic equation may lead to a more suitable quality assessment technique for micromoulding than the criteria currently used. In summary this technique provides a means for compressing point clouds representing surface features whilst providing an analytic description of such features. The work is applic-

able to many other instances where surface topography is in need of efficient representation.

Keywords: Surface profiling, micromoulding, Biharmonic equation.

---

1. Introduction

There are many materials for which the surface topography is a crucial characteristic. There are too many examples to list comprehensively, but a few instances serve to illustrate the range of materials and applications. One such is the work in [1] on surface geometry, wettability, roughness and other properties of composite polylactic acid and calcium phosphate glass scaffolds with a biological application. Another example whereby 3D shape characterization has been employed [2] involves a lunar soil simulant material with the aim of using the resulting shapes in a series of flow particle simulations. Some other examples include shape characterization of cement particles [3], characterization of ZnO [4], shape characterization of sol-gel zinc silicate glass particles [5] and large defects in alumina ceramics [6].

The above examples illustrate the relevance of shape characterization of particles or surfaces of a given material. However, shape characterization is also useful to describe or quantify the overall properties of manufactured parts such as the ones obtained through micromoulding.

Micromoulding refers to the mass production process through which devices with micro and nano scale surface features are manufactured [7] (the overall size of the components analyzed in this work is in the order of microns with nanometric surface features). This has become steadily more important over the past 30 years, when it was forecasted as one of the main manufacturing technologies of the 21^{st} century [8]. Its current relevance is mainly a byproduct of the constant development of portable electronic devices. This industry also manufactures devices for micro-optics, and life sciences applications. Most of the devices produced by this process are made of polymeric materials since this type of material offers the possibility of being tailored to the specific needs of a given application [8].

Micromoulding is affected by a number of variables such as the injection rate at which the moulding cavity is filled, injection and holding pressures, mould and melt temperature and cooling time [9]. Small variations in such variables may lead to a significant change in the shape and properties of the final product. Extensive research has been carried out on the influence that

these variables have on the final shape of the end product. These include studies on flow visualisation in micromoulding for determining cooling rates within the mould and research on the mechanical properties of micro components using Atomic Force Microscopy [10, 11, 12, 13]. Uncontrolled changes on the shape and properties of the component are clearly unwanted and quality control methods must be implemented. However, quality assessment techniques previously available, often applied to larger scale components, cannot offer the precision required to verify the quality of micromoulded components. Given that the product's functionality is directly related to its surface geometry, techniques that quantify the surface directly are desirable for the control of quality.

Research on product property measurement has been carried out and has been used to determine dimensional properties, consequently allowing for full three-dimensional assessments. Among the techniques readily available are:

- White Light Interferometry (WLI). This is a non-contact 3D surface measurement technique with an associated accuracy of fractions of a micron and is combined with an optical setup for visualizing structures at microscopic scales. It is set up in such a way that the height of a given two-dimensional point is determined by the relation between the path lengths of two different beams.

- Atomic Force Microscopy (AFM). The resolutions obtained with this technique are equivalent to fractions of a nanometer. The information is gathered via a probe with a very sharp nanometre sized tip and a sensitive piezoelectric actuator so that accurate small-scale scanning can be obtained. Its advantage over electron microscopy is that it provides a true three-dimensional profile, and that the instruments can perform in ambient conditions and even in liquids. [14], [13].

- Nanoindenting. This technique is so flexible that can be applied to different materials ranging from metals and plastics and in forms varying from thin films to powders [15]. A nanometre scale diamond tip is driven into the material surface with displacement and load monitored.

- Extensive Depth Of Field. The traditional optics concept of extensive depth of field has been applied within micromoulding as a technique for obtaining three-dimensional profiles by recording a number of images at different depths transversally to the focus plane. Then, the set of

images is processed so that a fully focused three-dimensional representation of the component is obtained [16].

- Utrasonic techniques, which combine the use of ultrasound and an optical laser to determine the dimensions of a given cavity [17].

In summary, surface measurement techniques employed for characterizing micro and nano scale surface features nowadays are generally associated with massive amounts of data in the form of three-dimensional point clouds. Management of these data is difficult in practice. Thus, a surface characterization technique capable of describing the surface geometry accurately whilst compressing the data set would be ideal.

This work proposes the use of Partial Differential Equations (PDEs) as means of obtaining a surface representation of a given micromoulded component semi-automatically. PDEs have been previously used as a surface generation technique to produce parametric surfaces in other generally larger scale applications and computer-aided design [18] and recently these authors have introduced PDEs as a surface generation technique for surface profiling of micro-scale structures [19]. Surfaces arising from PDEs are the graphic representation of the solution to a given PDE subject to a specific set of boundary conditions, translating surface characterization into a boundary-value problem. The boundary conditions describing outer contours of the surface are extracted from experimental point clouds. Periodic boundary conditions are used to ensure that analytic solutions can be found. Relevant design parameters are then expressed as functions of the coefficients describing the analytic solution to the Biharmonic equation, which can then be compared against the design values.

The proposed technique is graphically illustrated in Figure 1. This Figure shows a graphic representation of the overall process highlighting the most important steps associated with this technique. First, a component obtained through a micromoulding machine by filling a given mould is shown (Figure 1.a). Secondly, three-dimensional data representing the entire surface profile of such a component is obtained through WLI (Figure 1.b); this data being in the form of a point cloud. Thirdly, the profile is subdivided into regions representing each of the surface features that characterize the surface profile (Figure 1.c). Afterwards, a set of boundary curves are extracted from every subregion (Figure 1.d) and lastly, a PDE-based surface representation of each surface feature is obtained, followed by some quantitative analyses so that the the quality of the component can be determined (Figure 1.e).

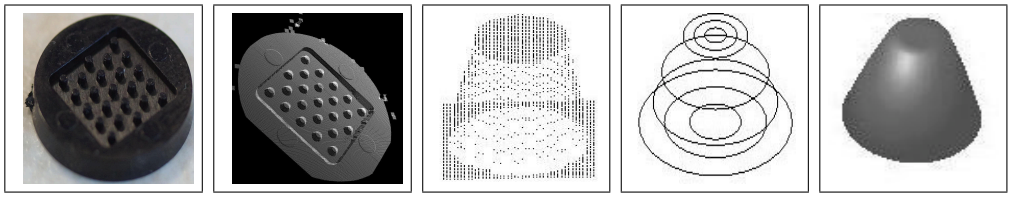

(a) (b) (c) (d) (e)

Figure 1: Schematic representation of the surface characterization process proposed in this work. The stages illustrated here start at the production of micromoulded components (a) followed by the extraction of three-dimensional data (b). These data are analyzed so that they are divided into regions representing each surface feature (c). Then, a set of boundary curves representing the surface profile of the feature is obtained (d) and the process finishes with the generation of a PDE surface representation of each surface feature within a given component (e).

Thus, a quality assessment method based on this comparison may be eventually incorporated into the production process. Moreover, this technique also allows the characterization of surface profiles with random or high frequency features and such a chracterization may prove useful for the study of some physical properties of such surfaces.

Note that the technique developed here is intended to compress the data contained in massive point clouds whilst finding an analytic expression for characterizing surface features. Also, it is worth highlighting the aim of the quality assessment method based on the use of this technique. This would be to provide an improved procedure for determining if the surface profile of the resulting manufactured micromoulded components is a sufficiently accurate representation of that originally intended.

This paper is organized as follows: Section 2 describes the mathematical foundations of the Biharmonic equation as a surface generation technique together with some graphical examples. This section also outlines the different curve extraction techniques employed throughout this work for characterizing micromoulding surface features. Section 3 provides several mathematical expressions relating relevant geometry parameters to the analytic solution to the Biharmonic equation for a particular surface feature. Section 4 presents the results obtained for different types of data sets representing a variety of micromoulding surface profiles and includes the analysis of different data sets representing the same surface profile as a prerequisite for generating an in-line quality assessment technique. Section 5 outlines the conclusions and

further directions of this work.

2. Solution of the Biharmonic equation as a surface generation technique

The use of elliptic PDEs as a surface generation technique was firstly applied to the area of computer aided geometric design as a technique suitable for blending surfaces [20]. However, the areas of application of such techniques have increased and include automatic design optimisation and interactive design [21] together with applications to physical and biological systems. The technique proposed here is based on the use of the Biharmonic equation as a surface generation technique, which has proved successful in Computer Aided Design (CAD) systems for representing complex shapes [21]. This is mainly due to the fact that it intrinsically offers tangential (C^1) continuity on every point of the resulting surface. Note that in order to guarantee curvature (C^2) continuity a sixth order elliptic PDE would be required and its solution can be found in a similar manner as the one used in this work.

The Biharmonic equation is an elliptic PDE often encountered in disciplines such as fluid and solid mechanics. This equation has been associated with suitable mathematical models for phenomena such as Stokes' flows, plane stress and plain strain problems in different geometries. Given the importance of this equation, several approaches have been undertaken to find its solution according to the nature of each specific problem. These techniques vary from pure analytic approaches to fully numerical techniques. This work uses an analytic solution that is valid when using periodic boundary conditions and is outlined below.

Nevertheless, it is important to stress that PDEs of different kinds and order may be used to generate surfaces. For instance, the work presented in [22] uses a sixth order elliptic PDE aiming to develop a fast surface modelling technique.

2.1. Analytic solution to the Biharmonic Equation

Surfaces arising from PDEs are often referred as PDE surfaces and in this work are defined as the graphic representation to the solution to the Biharmonic Equation over a two-dimensional parametric domain. The Biharmonic

equation is given by

$$\left(\frac{\partial^2}{\partial u^2}+\frac{\partial^2}{\partial v^2}\right)^2 \mathbf{X}(u,\,v)=0\,, \tag{1}$$

where u and v are the parametric surface coordinates, which are then mapped into the physical space through $\mathbf{X}(u,\,v):\mathbb{R}^2\rightarrow\mathbb{R}^3$; i. e.,

$$\mathbf{X}(u,\,v)=(x(u,\,v),\,y(u,\,v),\,z(u,\,v)).$$

A closed form analytic solution to Equation (1) in the form of a pseudo-spectral method can be found when restricting the boundary conditions to periodic ones and the parametric domain to $0\leq u\leq 1$ and $0\leq v\leq 2\pi$.

Thus, the particular solution to Equation (1) is found by specifying a set of four boundary conditions that define the value of $\mathbf{X}(u,\,v)$ and some of its derivatives at the boundary of the parametric domain. Note that due to the use of boundary conditions periodic in v, only four boundary conditions are required. Thus, the use of the Biharmonic equation as a surface generation technique requires two positional boundary conditions and their respective normal derivatives (in this particular case, the normal derivatives are equal to the derivatives with respect to u) at each respective edge of the domain.

For this particular technique and given that the boundary curves that are obtained from a given point cloud represent are positional boundary curves, the required derivative boundary conditions are found using standard finite differences techniques. That is, the positional boundary conditions are defined by the outermost curves at each respective edge of the surface patch and the inner ones are used to compute the corresponding derivative accordingly.

The solution is found using the method of separation of variables [23] and is given by,

$$\mathbf{X}(u,\,v)=\mathbf{A_0}(u)+\sum_{n=1}^{\infty}[\mathbf{A_n}(u)\cos(nv)+\mathbf{B_n}(\mathbf{u})\sin(nv)]\,, \tag{2}$$

where the vector-value polynomials $\mathbf{A_0}(u)$, $\mathbf{A_n}(u)$ and $\mathbf{B_n}(u)$ are determined by

$$\begin{aligned}
\mathbf{A_0}(u) &= \mathbf{a_{00}}+\mathbf{a_{01}}u+\mathbf{a_{02}}u^2+\mathbf{a_{03}}u^3\,, &(3)\\
\mathbf{A_n}(u) &= (\mathbf{a_{n1}}+\mathbf{a_{n3}}\mathbf{u})\,e^{anu}+(\mathbf{a_{n2}}+\mathbf{a_{n4}}u)\,e^{-anu}\,, &(4)\\
\mathbf{B_n}(\mathbf{u}) &= (\mathbf{b_{n1}}+\mathbf{b_{n3}}\mathbf{u})\,e^{anu}+(\mathbf{b_{n2}}+\mathbf{b_{n4}}u)\,e^{-anu}\,. &(5)
\end{aligned}$$

The value of the constant vectors $\mathbf{a_{ij}}$ and $\mathbf{b_{ij}}$ are determined by the specified boundary conditions, which, for this purpose, have to be expressed in terms of a Fourier series. Each of the components of these vectors corresponds to a direction in the Cartesian three-dimensional space.

Given that the general solution to the Biharmonic equation is expressed in terms of an infinite series, this solution needs to be approximated by a finite one whereby the first N terms of the sum are included together with the introduction of a remainder term. The approximation is given by,

$$\mathbf{X}(u,\, v) = \mathbf{A_0}(u) + \sum_{n=1}^{N} [\mathbf{A_n} \cos(nv) + \mathbf{B_n} \sin(nv)] + \mathbf{R}(u,\, v)\,, \tag{6}$$

where $\mathbf{R}(u,\, v)$ is a function defined as,

$$\mathbf{R}(u,\, v) = \mathbf{r_1}(v)e^{wu} + \mathbf{r_2}(v)e^{-wu} + \mathbf{r_3}(v)ue^{wu} + \mathbf{r_4}(v)ue^{-wu}\,. \tag{7}$$

The value of w has been conveniently chosen as $w = a(N+1)$ and, $\mathbf{r_1}(v)$, $\mathbf{r_2}(v)$, $\mathbf{r_3}(v)$ and $\mathbf{r_4}(v)$ are vector-valued functions denoting the difference between the original boundary conditions and the ones satisfied by,

$$\mathbf{F}(u,\, v) = \mathbf{A_0}(u) + \sum_{n=1}^{N} [\mathbf{A_n} \cos(nv) + \mathbf{B_n} \sin(nv)]\,. \tag{8}$$

Therefore, Equation (7) is responsible for exactly satisfying the original boundary conditions when using Equation (6). Note that in some particular cases all the original boundary conditions could be expressed in terms of finite Fourier series and, in such cases, the remainder term is not required.

Surface representations of objects with relatively simple topologies can be described using a single set of four boundary conditions. However, objects with more complex topologies often require more than one set of boundary conditions, leading to PDE-based surfaces composed of several surface patches. Each of these patches results from a solution to Equation 1 corresponding to its respective set of boundary conditions. Surface continuity is obtained by imposing common boundary conditions at the required region.

Examples of the different surface representations obtained using the Biharmonic equation are shown in Figure 2. The boundary curves used to solve the boundary-value problem are shown at the left of each respective surface. These examples correspond to some of the surface features that have been analyzed in this work.

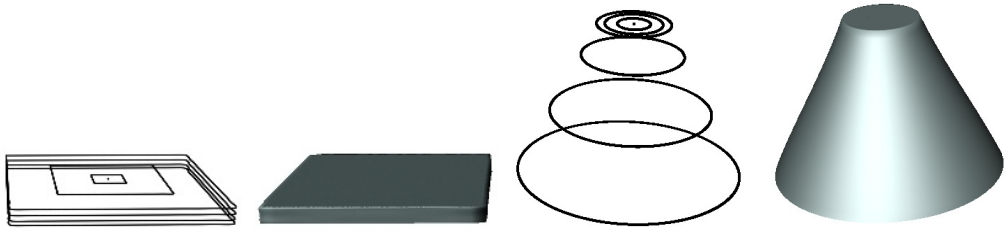

Figure 2: PDE-based surface representations of various objects. The boundary curves are outlined at the left whereas the corresponding PDE surface is shown at the right in each case.

Both; the boundary-value approach offered by the Biharmonic equation as a surface generation technique together with the parametric nature of the solution to this equation are ideal for compressing information stored in the form of massive point clouds such as the ones obtained. Therefore, PDE-based surface representations of micromoulding features may be obtained. Furthermore, key geometry parameters pertaining to a given surface feature can be expressed in terms of the coefficients associated with the particular solution to equation 6. Then, the values obtained by these expressions can be compared against the values originally assigned to the mould's geometry parameters, giving rise to a mechanism for determining the quality of all the components produced by the same mould.

Thus, in order to characterize micromoulding surface features using the Biharmonic equation, the appropriate number of boundary curves must be chosen. These curves are extracted from a point cloud as faithfully as possible so that they can describe the outer contour of the feature. This work employs two different curve extraction techniques. One is based upon a feature oriented approach whilst the other is aimed for representing full surface profiles. Naturally, the approach is selected according to each problem. Details on such techniques are given below.

2.2. Curve extraction procedure

The use of the Biharmonic equation as a surface characterization method for micromoulded surfaces is capable of drastically reducing the size of the data whilst maintaining crucial information associated with a surface profile of the corresponding component. To that end, boundary curves outlining the most important or prominent features must be extracted from the original data set. This results in adopting fairly straightforward procedures. One of

these curve extraction procedures is aimed at preserving the features observed and thus, the entire profile is divided into regions, the limits of which are based on the design of the mould.

By contrast, some of the profiles found in micromoulding are not directly associated with the component design. They may be characteristic of the process (e.g. extrusion) or the material. These profiles are particularly interesting since characterizing them may prove useful in understanding physical phenomena occurring during the process. For instance, surface profiles resulting from polymer blends present shapes often with random protuberances, which represent interface regions between the component materials. This type of surface profile requires a different curve extraction approach.

To that end, two different curve extraction techniques are used throughout this work. The first consists of extracting contours outlining a particular surface feature. This technique is particularly useful for feature-oriented analysis. Here, the subregions within the point cloud representing a given feature are further divided into subregions representing slices or transversal subregions. The extraction process consists of identifying the closest points to a pre-defined template (subject to a tolerance value that is adjusted manually). The final boundary curves are then found by averaging the position of the identified points within the area to which they belong according to the pre-established template. The second curve extraction approach used throughout this work is based on representing the entire profile of a micromoulding component. Here, a number of transversal curves are obtained from the point cloud. Note that in order to satisfy the periodicity condition inherent to the specific analytic solution to the Biharmonic equation in use through out this work, the transversal curves must be closed.

In summary, the boundary curves required to find a PDE-based representation of the surface profiles analyzed in this work were extracted either by using a pre-determined template outlining the contour of a specific feature or by extracting transversal curves at specified positions along the surface. It is worth noting that some of these curves are used to determine the derivative boundary conditions by using finite differences.

Examples of the two different curve extraction approaches are shown in Figure 3. The left hand side of the Figure show the boundary curves associated with features found in a typical silicon-made calibrating grid (Figure 3.a) whereas the right hand side shows transversal curves extracted from the profile of a 30 nm thick layer of poly(N-isopropylacrylamide), on a Sylgard (TM) silicone elastomer substrate (Figure 3.b).

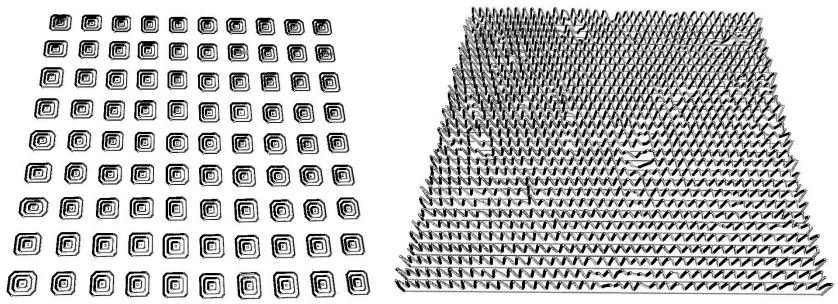

(a) (b)

Figure 3: Curve extraction techniques. Feature oriented approach (a) and transversal set of curves (b).

3. Design parameter characterization as a function of the solution to the Biharmonic equation

Typically the surface topography of the component will correspond to a particular design, but will replicate it imperfectly. The design from where micromoulded components are obtained is intrinsically associated with a number of parameters (geometry parameters henceforth), which are specified so that the particular engineering requirements of a given mould are met. For instance, a component presenting a cylindrical surface feature is associated with two geometry parameters: radius and height of the cylinder. Therefore, a methodology for determining the experimental values of such parameters is highly desirable. On the other hand, the coefficients associated with the analytic solution to the Biharmonic equation given in Equation 6 are in their own right a different set of parameters representing the shape of the surface of each particular feature.

Thus, a mechanism for measuring the value of the geometry parameters for the micromoulded components can be implemented. The experimental value of the geometry parameters found as a byproduct of the coefficients (PDE coefficients henceforth) involved in Equation 6 can be then compared against the mould design values themselves. To that end, expressions relating geometry parameters to the PDE coefficients must be found.

It is important to stress that closed surface representations are obtained by solving at least three PDEs, each of which is subject to a different set of boundary conditions; however, the boundary conditions are chosen so that C^0 continuity is guaranteed. Two of these PDEs are responsible for closing

the surface; that is, the overall shape of the surface representing the feature has no holes and consequently, the volume enclosed by the surface can be computed numerically. Thus, a minimum of three different sets of PDE coefficients are available for characterizing geometry parameters defining a surface feature. Let the set of solutions associated with a given surface feature be represented by

$$\chi_{[i]}(u,v) = A_{0[i]}(u) + \sum_{n=1}^{n=N} \left[A_{n[i]}(u)\cos(nv) + B_{n[i]}(u)\cos(nv) \right]. \qquad (9)$$

where $i = 1, \ldots, k$ represent the corresponding surface patch. Table 1 shows the formulae relating some of the most relevant geometry parameters to the PDE coefficients according to a particular surface feature.

Note that the features and their respective geometry parameters in Table 1 are examples, which have been chosen for illustration purposes and do not represent a limit on the potential of the Biharmonic equation for characterizing surface features.

3.1. Standard quality criterion

So far, the criteria used to determine the quality of manufactured micromoulding components consist of imposing a threshold to some geometry parameters. The components are regarded as good if the component meets the pre-established threshold, otherwise the component is then regarded as faulty. However, the methods for evaluating such geometry parameters during the in-line production process are crude. The same type of criteria is used in this work, with the difference that the value of the geometry parameter with a pre-established threshold is found through an expression depending upon the PDE coefficients. Thus, a more robust method involving the complete area of interest for that particular parameter is included.

4. Results

The technique developed here has been tested using experimental data arising from both WLI and AFM. The only difference this makes to the proposed technique lies with the way in which the data is pre-processed so that the curve extraction procedure can take place.

Table 1: Characterization of relevant geometry parameters in terms of PDE coefficients according to different shapes of possible surface features.

Feature shape	Geometry parameters	Expression relating geometry parameters to PDE coefficients
Circular cylindrical surface	base radius, r height, h	$r = \|A_{1[2]}(0) - A_{0[2]}(0)\|$ $h = \|A_{0[2]}(1) - A_{0[2]}(0)\|$
Elliptic cylindrical surface	major base radius, a minor base radius, b height, h	$a = \|A_{1[2]}(0) - A_{0[2]}(0)\|$ $b = \|B_{1[2]}(0) - A_{0[2]}(0)\|$ $h = \|A_{0[2]}(1) - A_{0[2]}(0)\|$
Quadrilateral prism	side a side, b height, h	$a = 2\|\chi_{[2]}(0, \frac{\pi}{2}) - \chi_{[2]}(0, 0)\|$ $b = 2\|\chi_{[2]}(0, \pi) - \chi_{[2]}(0, \frac{\pi}{2})\|$ $h = \|A_{0[2]}(1) - A_{0[2]}(0)\|$
Conical cylindrical surface (circular)	base radius, a top radius, b height, h	$a = \|A_{1[2]}(0) - A_{0[2]}(0)\|$ $b = \|A_{1[2]}(1) - A_{0[2]}(1)\|$ $h = \|A_{0[2]}(1) - A_{0[2]}(0)\|$
Conical cylindrical surface (elliptical)	base major radius, a_1 base minor radius, b_1 top major radius, a_2 top minor radius, b_2 height, h	$a_1 = \|A_{1[2]}(0) - A_{0[2]}(0)\|$ $b_1 = \|B_{1[2]}(0) - A_{0[2]}(0)\|$ $a_2 = \|A_{1[2]}(1) - A_{0[2]}(1)\|$ $b_2 = \|B_{1[2]}(1) - A_{0[2]}(1)\|$ $h = \|A_{0[2]}(1) - A_{0[2]}(0)\|$
Parabolic nose cone	major semi-axis, a minor semi-axis, b height, h	$a = \|A_{1[2]}(0) - A_{0[2]}(0)\|$ $b = \|B_{1[2]}(0) - A_{0[2]}(0)\|$ $h = \|A_{0[2]}(1) - A_{0[2]}(0)\|$
Collection of n concentric circular cylinders	base radii, $r_i, i =, \ldots, n$ height, h	$r_i = \|A_{1[2i]}(0) - A_{0[2i]}(0)\|$ $h_i = \|A_{0[2i]}(1) - A_{0[2i]}(0)\|$

For instance, the data obtained through AFM is originally collected in a two-dimensional format. The resulting two-dimensional image is analysed so that the light intensity of each pixel is transformed into the height associated with the coordinates of that particular pixel. Thus, three-dimensional information representing the overall surface profile of a given component is generated.

By contrast, experimental data obtained using WLI is already in three-dimensional form. However, these data sets may contain some points for which no reading of its corresponding height could be recorded. To that end, faulty points are removed form the data set.

After either converting the data into a three-dimensional point cloud or removing incomplete information, a suitable curve extraction process is employed according to the approach needed for characterizing each particular profile.

4.1. AFM experimental data

Different AFM data sets representing various micromoulding components have been analysed. Two of these data sets correspond to a silicon calibrating grid and a third one is associated with a 30 nm thick layer of poly(N-isopropylacrylamide), on a Sylgard (TM) silicone elastomer substrate (PNIPA surface henceforth). Figure 4 shows the two-dimensional image of the three data sets corresponding to the silicon calibrating grid at two different magnifications (Figure 4.a and Figure 4.b) and to the PNIPA surface (Figure 4.c) respectively . Note that the first data set representing the calibrating grid comprising 90 complete surface features whilst the second one contains four complete surface features.

The full three-dimensional representation of these data sets is shown in Figure 5. These boundary curves associated with each data set have been extracted accordingly. Thus, the data sets pertaining to the calibrating grid have been processed using the feature-based approach whilst the boundary curves associated with the PNIPA surface have been obtained using the profile-oriented method. Each of the features in these data sets has been represented using 10 boundary curves. This enables us to obtain closed PDE-based surface representations of each feature and allow to compute its volume. The boundary curves extracted for the data sets representing the calibrating grid together with the corresponding PDE-based surface representations are presented in Figure 6.

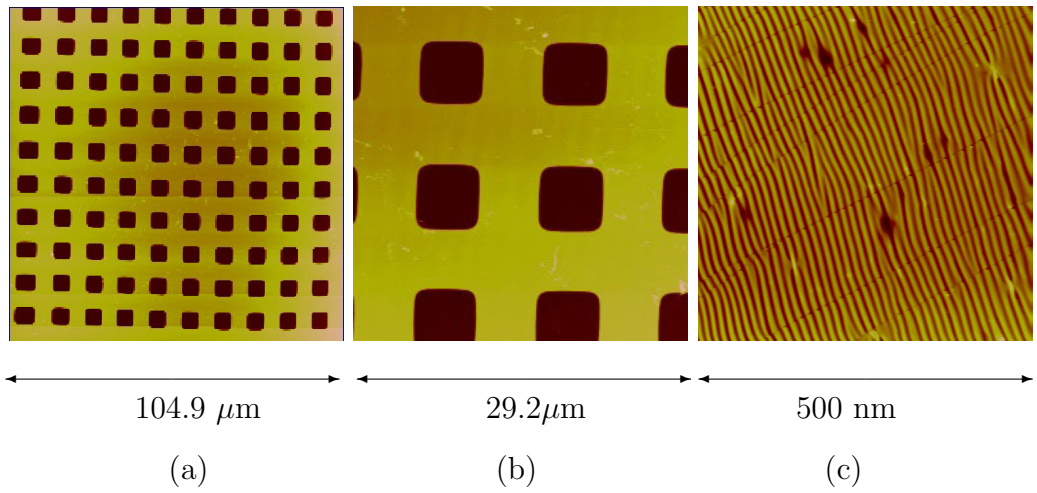

Figure 4: Experimental data obtained using Atomic Force Microscopy. Two sets corresponds to a silicon calibrating grid((a) and (b)), whereas the third represents an PNIPA surface surface (c).

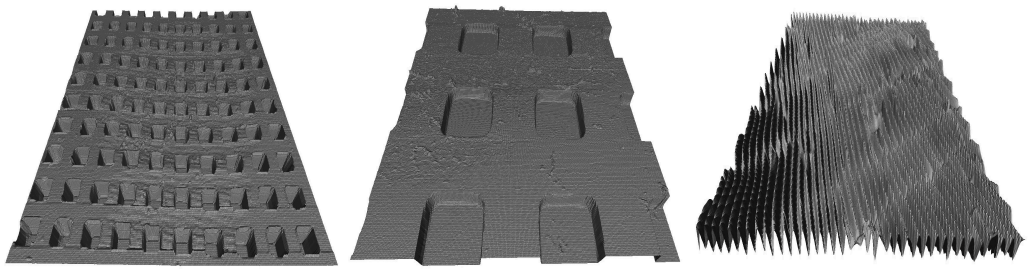

Figure 5: Three-dimensional representation of the complete data sets representing a calibrating grid and the surface profile of a PNIPA surface accordingly.

Then, once the boundary curves are extracted, the corresponding PDEs are solved, leading to a set of coefficients for each PDE being found and also the PDE-based surface representation of the corresponding surface feature being obtained. Thus, the geometry parameters associated with these features have been found using the respective PDE coefficients and the corresponding formulae as described in Table 1 for quadrangular prisms. The average length of the side and the height found after analysing the data set comprising 90 surface features have been found to be equal to 4.82 μm for the side length whereas the height presented a value of 345.79 nm. By contrast, the values for the same design parameters after analysing the data

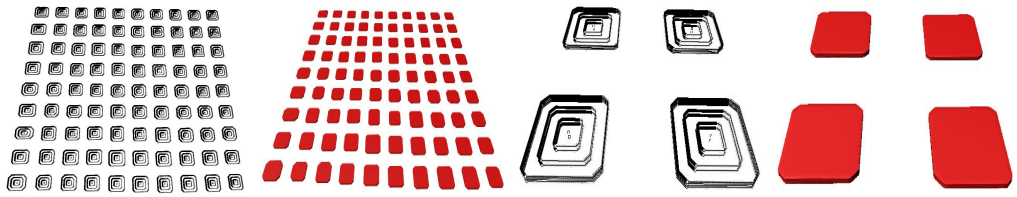

Figure 6: Boundary curves and the corresponding PDE-based surface representation of surface features present in a calibrating grid. Two different data sets at different scales are shown.

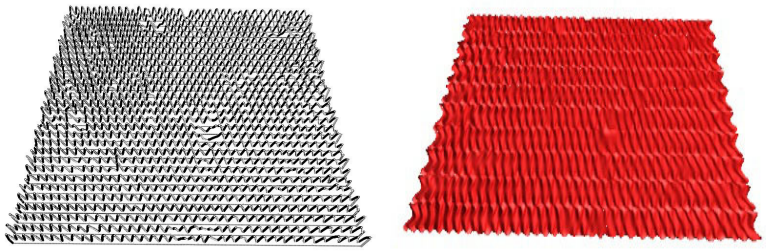

Figure 7: Boundary curves extracted form a data set representing the surface profile of a PNIPA surface. The resulting PDE-surface representation is shown at the right.

set describing four complete surface features were found equal to 5.086 μm and 348.05 nm respectively. The two data sets represent the same surface features at different scales, the average values closer to the ones with which the calibrating grid was designed (a side length equal to 5μm and a height equivalent to 350 nm) are those obtained from the data set portraying four surface features. This can be attributed to the gain in pixel resolution with magnification.

By contrast, the boundary curves required for obtaining a PDE-based surface representation of the surface profile of PNIPA surface have been extracted so that the entire profile is described. This helps to preserve the original nature of such a profile. Thus, a total of 31 curves have been extracted equidistantly along the profile. These curves give rise to a PDE-based surface representation composed of a total of 10 PDEs. Figure 7 presents the generating boundary curves and the corresponding PDE-based surface representation.

Given that no geometry parameters are associated with surface profiles arising from this type of surfaces, different properties can be used to characterize the profile. Thus, in the interest of taking advantage of the dependency

between the surface's functionality and the surface area, PDE-based surface representations of such profiles may be used to compute their surface area. The surface area of the profile used here has been found using numerical techniques and has been found equal to 6.07 x 10^8 [nm^2]. Therefore, PDE-based surface representations have proven to be useful for characterizing important physical properties of complex profiles by providing a mechanism for quantifying their surface area in a fast and accurate manner. Moreover, these PDE-based surface representations of this type of profile may provide excellent means for multi-scale analyses of more complex surface profiles.

4.2. WLI experimental data

Data obtained using WLI have also been characterized using PDE surfaces. The data sets analyzed here consist of six different samples representing different components obtained using the same mould. A picture of one of the components is presented in Figure 1.a. This component has been manufactured using Bayer Makrolon LED 2045 polycarbonate with 1 wt% multi-wall carbon nanotubes and consists of 23 circular cylindrical surface features with nominally uniform height and the nominally equal base and top radii. Faulty points present within the raw-data obtained through WLI were removed from each data set and profiles similar to the one presented in Figure 1.b were obtained. Note that each of these three-dimensional profiles is composed of more than half a million points and consequently a PDE-based characterization of the entire profile using a small portion of these data is ideal.

A feature-oriented curve extraction approach has been adopted for obtaining the necessary boundary curves for generating a closed PDE surface representation of each of the features in each data set. To that end, a semi-automatic procedure has been implemented. The first stage of that procedure consists of sectioning the full data set so that each section contains enough information so that each feature can be characterized. Then, the corresponding boundary curves are generated according to the type of surface that is required; that is, open or closed. An example of shown region is illustrated by Figure 1.c whilst the set of boundary curves found for that features are shown in Figure 1.d.

Figure 8 presents all the boundary curves for all of the cylindrical surface features present within each data set. The resulting PDE-based surface representations of each of the components are presented in Figure 9 accordingly. Closed surface representations for each of the features have been produced

here so that the surface area and volume associated with each feature can be computed. By simple inspection, it can be noticed that one surface feature in the sixth data set presents a height significantly smaller than that of the rest of the surface features. The formulae describing the geometry parameters associated with these surface features in terms of PDE coefficients are given in Table 1. The average value for the base and top radii together with the average height of the features present in each data set are then found. Additionally, average values for surface area and volume have been estimated.

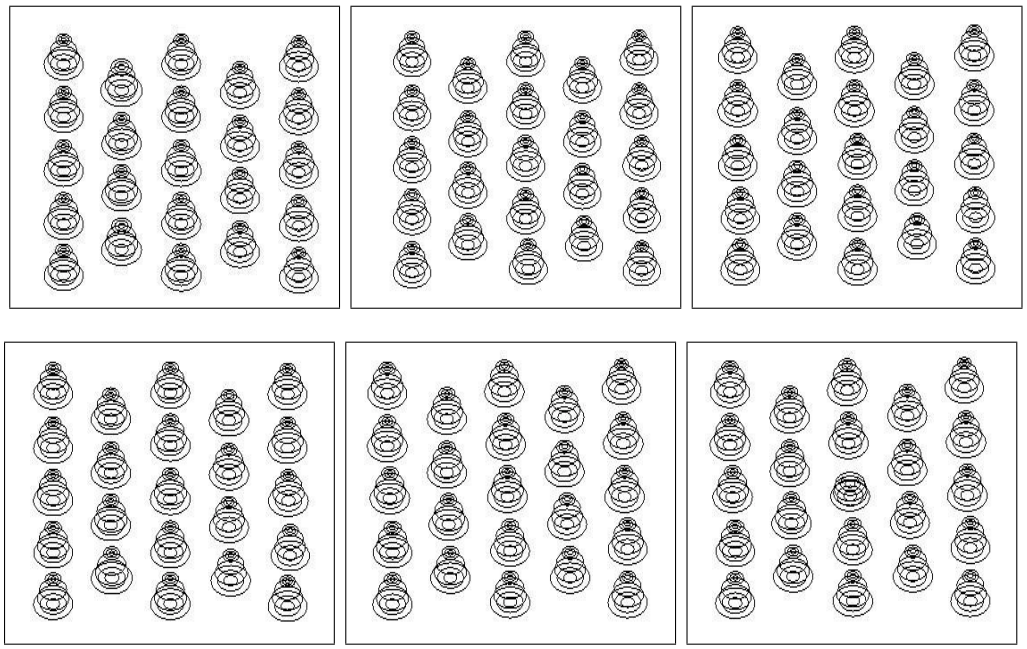

Figure 8: Boundary curves representing each of the cylindrical surface features of different components obtained from the same mould.

Table 2 presents the average radii and height found for each data set. These were obtained by using the PDE coefficients representing each surface feature. Additionally, the average total surface area associated with each data set is listed in this Table. The design values assigned to the base and top radii are 300 μm and 225 μm respectively. It is noticed that the base radii have been overestimated whereas the top radii have been underestimated. This tendency can be explained by the fact that boundary conditions represent outer contours delimiting the surface feature. Thus, given the nature of the

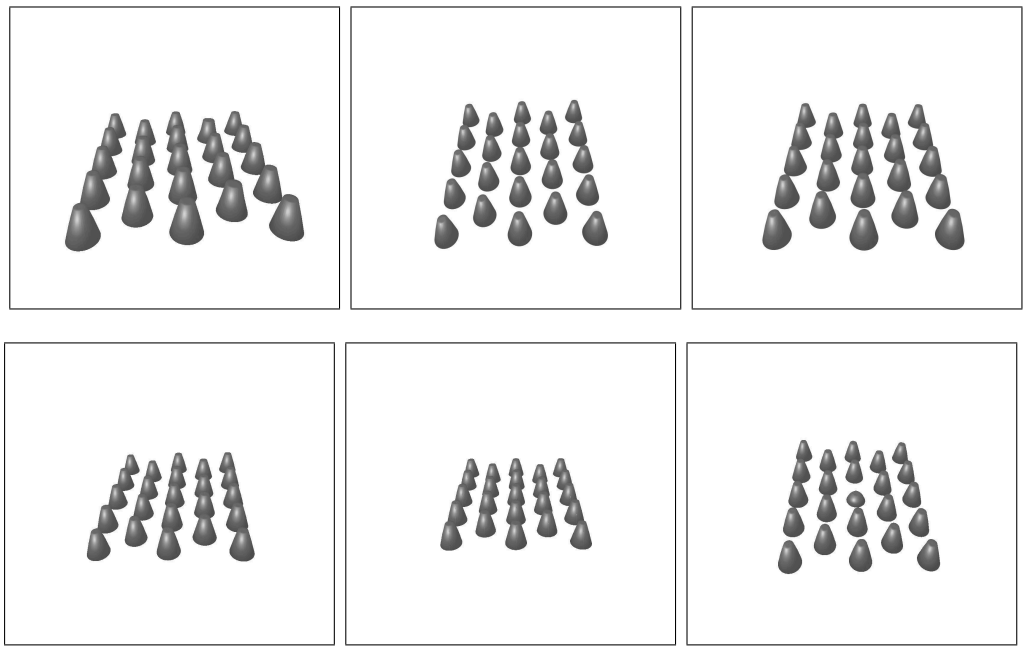

Figure 9: Resulting PDE-Based surfaces of all the cylindrical surface features present with each of the components.

profile, it can be seen that the curve representing the base radius of each surface feature is found by averaging a set of points approaching it from the outer limit of the feature. By contrast, the boundary curve associated with the top radius is found by averaging a set of points delimiting the top radius of each feature from the inner limit.

The design value assigned to the height of the surface features is 600 nm. Again, the average height of the surface features found for each sample presents a slight underestimation of approximately 25 nm. However, this underestimation is within the standard tolerance value. The criterion used to determine the quality of these components involves establishing a threshold value for the height. Thus, the height of each surface feature within a component is compared against the threshold value (550 nm) and if one of the surface features does not meet this requirement, the component is regarded as faulty. The six samples analysed throughout this work have been subject to this procedure and it has been found that one of the features in the sixth data set presented a considerably smaller height (225 nm) than the threshold. Therefore, the component associated with this data set must be regarded as

faulty.

Table 2: Average design values obtained using the PDE-based representation of the surface features present within each data set. Average total surface area and volume are also listed for each data set.

Sample	Average base radii r_b [μm]	Average top radii r_t [μm]	Average height h [nm]	Average surface area x10^8 [nm]^2	Average volume x10^{11} [nm]^3
1	343.63	143.37	564.25	1.35	1.34
2	343.33	139.23	571.00	1.35	1.38
3	342.82	136.67	569.43	1.34	1.36
4	345.77	141.68	567.88	1.36	1.38
5	342.24	144.24	568.54	1.37	1.40
6	343.96	144.00	554.03	1.35	1.36

Table 3 shows the original data size, the boundary and PDE information data size together with the compression rates potentially achieved by the technique proposed here on each respective data set included in this work. Compression rates of at least 66 % have been found suggesting that this PDE-based methodology would be very efficient for characterizing micro and nano-scale surface features of micromoulded components.

Table 3: Data size and compression rates associated with each of the cases considered in this work.

Experimental data set	Original data size [kB]	Boundary data size [kB]	PDE data size [kB]	Compression rate [%]
Full calibrating grid	5, 598	1800	60.480	66.77
Section of calibrating grid	5,601	80	2.688	98.52
PNIPA surface	2,465	594	6.720	75.63
Sample 1	12,126	460	19.8	99.84
Sample 2	11,999	460	19.8	99.83
Sample 3	12,499	460	19.8	99.84
Sample 4	11,913	460	19.8	99.83
Sample 5	11,992	460	19.8	99.83
Sample 6	12,262	460	19.8	99.84

5. Conclusions

Parametric representations of micro and nano scale surface features have been obtained using PDEs. This characterization has taken place using the Biharmonic equation as a surface generation technique, which can be solved analytically when its boundary conditions are restricted to periodic ones. This enables us to significantly reduce the size of data sets generally associated with micromoulding since relevant features within a given profile can be represented by a relatively small set of boundary conditions. The coefficients associated with the particular analytic solution of the Biharmonic equation for a given surface profile have proven useful for characterizing geometry parameters of surface features present within a given component as a function of either some of the coefficients or the full solution itself. Experimental data obtained by using different techniques, namely AFM and WLI, have been analysed in order to show that the PDE-based surface generation technique proposed here can be applied indiscriminately once the data is in three-dimensional form.

Two AFM data sets representing a silicon calibrating grid at different optical scales have been analysed throughout this work. The quadrangular features observed in the grid were characterized using the PDE-based approach proposed here and it was found that the side length and height found for the set with 90 complete surface features are equal to 4.82 μm and 345.79 nm on each respective case, whilst the data set representing four complete surface features presents a side length equal to 5.086 μm and a height of 348.05 nm. The discrepancy in these values is expected since the values found for the data set with four complete surface features are essentially a refinement of the measurement of a particular area within the grid. Additionally, an AFM surface profile of a PNIPA surface was characterized using the Biharmonic equation. To that end, transversal curves along the entire profile were extracted and a total of 10 PDEs were solved. The resulting PDE surface representation was used to calculate the total surface area of the profile, which has been found equal to 6.07 x 10^8 [nm^2]. This suggests that the surface generation technique adopted here may provide means for characterizing physical properties describing the surface's functionality that depend on the surface area.

Six samples of WLI of experimental data representing different components obtained from the same mould have been analysed. The surface features present in these components presented a circular cylindrical shape with dif-

ferent base and top radii. A procedure for extracting the necessary boundary curves was implemented so that they could be extracted semi-automatically. The coefficients associated with each feature were then employed to find the values of the geometry parameters associated with this shape. Thus, it has been found that the PDE-based technique developed here can be potentially implemented in the production line as a quality assessment technique since it has been shown that it can detect features that do not meet the minimum requirements imposed for certain design parameters. However, either an overestimation or otherwise was noticed for some design parameters. This is seen as an artifact of the semi-automatic curve extraction procedure, which can be eliminated if some refinements of such procedures are imposed.

This work is intended to be continued so that the methodology proposed here can be fully implemented within the in-line production procedure. To that end, the first aim is to refine the curve extraction methodology by adding some criteria so that the algorithm responsible for averaging the experimental data can weight each point according to some guidelines, which reflect on the critical importance of certain measurements. Furthermore, PDE-based surface profiles of polymer-blend surfaces will be used to determine physical properties of larger scale surfaces. This will be carried out using a multi-scale approach with numerical techniques for describing properties such as thermal contact resistance or heat transfer.

Acknowledgements

We wish to acknowledge Dr Peter Twigg, of the School of Engineering, Design and Technology, for the AFM measurement on PNIPA. Additionally, we wish to acknowledge the support received from the UK Engineering and Physical Science Research Council grant EP/G06573X/1 through which this work was completed.

References

[1] M. Charles-Harris, M. Navarro, E. Engel, C. Aparicio, M. P. Ginebra, J. A. Planell, Surface characterization of completely degradable composite scaffolds, Journal of Materials Science: Materials in Medicine 16 (12) (2005) 1125–1130.

[2] T. Matsushima, J. Katagiri, K. Uesugi, A. Tsuchiyama, T. Nakano, 3D shape characterization and image based DEM simulation of the lunar soil simulant FJS-1, Journal of Aerospace Engineer 22 (1) (2009) 15–23.

[3] S. T. Erdoğan, X. Nie, P. Stutzman, E. J. Garboczi, Micrometer-scale 3-D shape characterization of eight cements: Particle shape and chemistry and the effect of particle shape on laser diffraction particle size measurement, Cement and Concrete Research 40 (5) (2010) 731–739.

[4] H. Chang, M. Tsai, Synthesis and characterization of ZnO nanoparticles having prism shape by a novel gas condensation process, Advances in Technology of Materials and Materials Processing 18 (8) (2008) 734–743.

[5] J. Xu, E. S. O'Keefe, C. C. Perry, The preparation and characterization sol-gel zinc silicate glass particles with pramid shape and millimetre size, Journal of Materials Chemistry 14 (2004) 1744–1748.

[6] K. Sato, S. Tanaka, N. Uchida, K. Uematsu, Novel characterization procedure of large defect in ceramics, Advances in Technology of Materials and Materials Processing 2 (1) (2004) 63–68.

[7] L. Weber, W. Ehrfeld, Micromoulding market position and development, Kunsttoffe Plast Europe 89 (10) (1999) 192–202.

[8] K. J. Gabriel, Engineering microscopic machines, Scientific American: Technology in the 21st Century, 150th Anniversary Issue 273 (3) (1995) 150–153.

[9] S. Sha, S. Dimov, C. Griffiths, M. Packianather, Investigation of micro-injection moulding: Factors affecting the replicating quality, Journal of Materials Processing Technology 183 (2) (2007) 284–296.

[10] J. Zhao, R. H. Mayes, C. Ge, X. Hong, P. S. Chang, Effects of process parameters on the micro moulding process, Polymer Engineering and Science 43 (9) (2003) 1542–1554.

[11] B. R. Whiteside, M. T. Martyn, P. Coates, G. Greenway, P. Allen, P. Hornsby, Micromoulding: Process, characteristics and product properties, Plastics, Rubber and Composites 33 (1) (2004) 11–17.

[12] B. R. Whiteside, R. Spares, K. Norris, P. D. Coates, Influence of mould design on flow visualisation studies in micromoulding, Proc. Polymer Process Engineering 09 (2009) 249–262.

[13] M. Kobayashi, C. K. Jen, Piezoelectric thick bismuth titanate/lead zirconate titanate composite film transducers for smart NDE of metals, Smart Materials and Structures 13 (2004) 951–956.

[14] F. J. Giessibl, Advances in atomic force microscopy, Rev. Mod. Phys. 75 (3) (2003) 949–983.

[15] A. A. Volinsky, W. W. Gerberich, Nanoindentation techniques fro assessing mechanical reliability at the nanoscale, Microelectronic Engineering 69 (2-4) (2003) 519–527.

[16] B. R. Whiteside, R. Spares, P. Coates, In-process 3D assessment of micromoulding features, Optical Micro- and Nanometrology in Microsystems Technology 6188 (1) (2006) 61880Z.

[17] Y. Ono, et al, Real time non-intrusive and non-destructive ultrasonic monitoring of injection and co-injection molding processes, Proc. Society of Plastics Engineers ANTEC (2004) 556–560.

[18] G. González Castro, H. Ugail, P. J. Willis, I. J. Palmer, A survey on partial differential equations in geometric design, The Visual Computer 24 (3) (2008) 213–225.

[19] G. González Castro, R. Spares, H. Ugail, B. R. Whiteside, J. Sweeney, Surface profiling of micro-scale structures using partial differential equations, International Journal of Material forming 3 (Supplement 1) (2010) 415–418.

[20] M. I. Bloor, M. J. Wilson, Generating blend surfaces using partial differential equations, Computer Aided Design 21 (3) (1990) 165–171.

[21] H. Ugail, M. I. Bloor, M. J. Wilson, On interactive design using the pde method, Proc. Mathematical Methods for Curves and Surfaces II (1998) 493–500.

[22] J. J. Zhang, L. You, Fast Surface Modelling using a 6th Order PDE, Computer Graphics Forum 23 (3) (2004) 311–320.

[23] R. Courant, D. Hilbert, Methods of Mathematical Physics, Vol. 2, New York: Interscience, 1962.